Physical and electronic structure and magnetism of Mn_2NiGa: Experiment and density-functional theory calculations

G. D. Liu, X. F. Dai, S. Y. Yu, Z. Y. Zhu, J. L. Chen, and G. H. Wu
Beijing National Laboratory for Condensed Matter Physics, Institute of Physics, Chinese Academy of Sciences, Beijing 100080, People's Republic of China

H. Zhu and John Q. Xiao
Department of Physics and Astronomy, University of Delaware, Newark, Delaware 19716, USA
(Received 16 May 2006; revised manuscript received 20 July 2006; published 31 August 2006)

Both experimental and theoretical studies have been carried out to study the structure and magnetic properties of Mn_2NiGa alloys. We have found, instead of forming $L2_1$ structure where both *A* and *C* sites are occupied by Mn atoms, the alloy favor a structure where the *C* site is occupied by Ni atoms and Mn atoms at *A* and *B* sites. The electronic structures of both cubic austenite and tetragonal martensite Mn_2NiGa were calculated by self-consistent full-potential linearized-augmented plane-wave (FP-LAPW) method. Austenite Mn_2NiGa materials show ferrimagnetism due to antiparallel but unbalanced magnetic moments of Mn atoms at *A* and *B* sublattices. The magnetic moment of Mn atoms decrease greatly upon martensitic transformation to a tetragonal structure with a 50% reduction in Mn moments at the *A* site and almost completely suppressed Mn moments at *B* sites. Consequently, martensite Mn_2NiGa alloys show ferromagnetic coupling. Different magnetic orderings in martensite and austenite also lead to very different temperature dependence, with which the abnormal behavior of magnetization upon martensitic transformation can be understood. In the off-stoichiometric samples with composition between Ni_2MnGa and Mn_2NiGa, we show that additional Mn atoms that substitute for Ni atoms in Ni_2MnGa have the same magnetic behaviors as Mn in Mn_2NiGa phase, which successfully explains the dependence of the magnetization on Mn composition.

DOI: 10.1103/PhysRevB.74.054435 PACS number(s): 75.50.Cc, 71.20.Lp, 64.70.Kb, 71.15.−m

I. INTRODUCTION

The Heusler alloys first became of interest in 1903 when F. Heusler discovered that it is possible to make ferromagnetic alloys entirely from non-ferromagnetic elements.[1,2] Heusler alloys are ternary intermetallic compounds with highly ordered $L2_1$ structure, which belongs to the $Fm\bar{3}m$ space group. The structure has 16 atoms in a unit cell and is best described in terms of four interpenetrating fcc sublattices *A*, *B*, *C*, and *D* as shown in Fig. 1(a).[2,3] Based on the different alignments of *X*, *Y*, and *Z* atoms in four fcc sublattices, different ordered structures can be obtained.

Ferromagnetic shape memory alloy (*FSMA*) Ni_2MnGa is a typical Heusler alloy with *A* and *C* sites being occupied by Ni atoms, and *B* and *D* sites by Mn and Ga atoms respectively. The large Mn-Mn distance of 4.12 Å suggests that the indirect exchange between Mn atoms dominates in Ni_2MnGa.[2–4] Both theoretical and experimental results indicate that Mn atoms, instead of the Ni atoms, are the main contributors to the magnetism in Ni_2MnGa.[3,4] Large local Mn magnetic moments also lead to high saturation magnetization in this material. The materials have also been extensively studied with many reports on their structure, magnetic properties, martensitic transformation, magnetically controlled shape memory effect, and magnetic-field-induced strain.[5–9] In order to develop new FSMAs based on Ni_2MnGa, many works have been performed on the off-stoichiometric Ni_2MnGa which revealed some interesting results.[10–23] The magnetic properties and martensitic characteristics of $Ni_{2-x}Mn_{1+x}Ga$ alloys were found to change dramatically when additional (*x*) Mn substitutes for Ni.[24,25] It's believed that the moments of these additional Mn atoms are aligned antiparallel to those of the original Mn atoms.[24] However, the structure and magnetic properties in the Ni-Mn-Ga system with Mn content higher than 40 at. % have

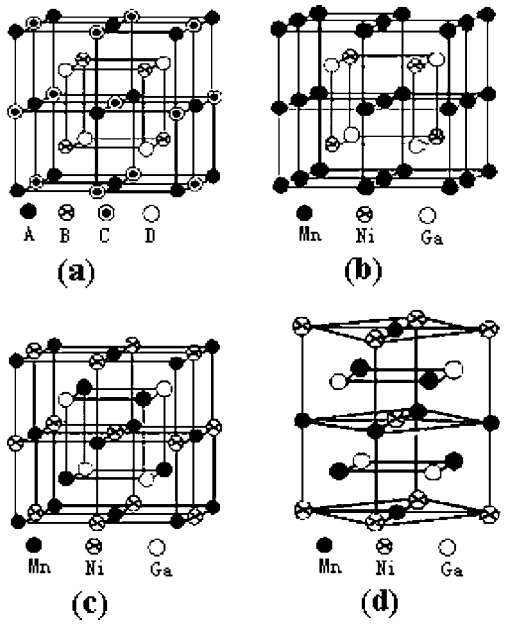

FIG. 1. (a) The generalized Heusler structure with four interpenetrating fcc sublattices *A*, *B*, *C*, and *D*. (b) Unit cells of the Mn_2NiGa with cubic MnNiMnGa ($L2_1$) structure, and (c) MnMnNiGa structure. (d) Unit cells of the Mn_2NiGa with tetragonal MnMnNiGa structure in the (110) direction.

rarely been studied. Recently, we reported that Mn_2NiGa alloy exhibits a martensitic transformation around room temperature and an excellent two-way shape memory behavior with a strain of 1.7% in single crystal samples.[26] In this paper, we will focus on Ni-Mn-Ga system with high Mn content and study the structure and magnetic properties of Mn_2NiGa alloys synthesized in our previous work. The Mn_2NiGa alloy is found to have a cubic structure with the saturation magnetization of about 33.49 emu/g. In this structure, Mn atoms prefer the *B* sublattice, while Ni atoms prefer the *A* or *C* sublattices. Our theoretical calculations show the Mn magnetic moments ($2.52\mu_B$) at *A* sites are antiparallel to the Mn moments ($3.56\mu_B$) at *B* sites, thus forming ferrimagnetic structure in austenite phase. The magnetic properties change dramatically through the martensitic transformation to a tetragonal structure with reduced Mn moment of $1.44\mu_B$ at *A* sites and almost diminishing Mn moments of $0.02\mu_B$at *B* sites. Consequently, Mn_2NiGa alloy shows ferromagnetic behavior in the martensite phase. In the following, we will discuss details of both theoretical and experimental studies of these properties.

II. EXPERIMENTAL AND COMPUTATIONAL DETAILS

The samples studied in this work were prepared by arc melting Ni, Mn, and Ga with purity of 99.95% in an argon atmosphere and a water-cooled Cu crucible. The arc-melted samples were encapsulated in quartz tube filled with argon, annealed at 1073 K for 72 h, and subsequently quenched into an ice-water mixture. The structure of the samples was determined using powder x-ray diffraction (XRD). The low temperature saturation magnetizations (M_s) were measured using a superconducting quantum interference device magnetometer (SQUID) in fields up to 5 T. The high temperature saturation magnetization was measured by a vibrating sample magnetometer (VSM).

The electronic structure of Mn_2NiGa was calculated using the self-consistent full-potential linearized-augmented plane-wave (FP-LAPW) method based on the local spin-density approximation within the density functional theory,[27,28] where the potential and/or the charge density in the crystal are treated with no shape approximation. Sixty *k* points for the austenite and 80 *k* points for the martensite in the irreducible Brillouin zone turn out to be sufficient for the results presented in this paper (0.1 mRy for the total energy per cell). The self-consistent calculation stops as the charge density deviation is less than 0.01 me/a.u. and the total energy deviation is better than 0.1 mRy per cell. The experimental lattice constants are used in the calculation. The muffin-tin sphere radii *R* used are 2.3 a.u. for Mn and 2.4 a.u. for Ni and Ga atoms. The density plane-wave cutoff is $Rk_{\max}=8.0$. The electron states were treated in a scalar relativistic approximation. Using the energy eigenvalues and eigenvectors at these points, the density of states was determined by the tetrahedral integration method.[29]

III. RESULTS AND DISCUSSIONS

A. Structure

The chemical structure of the Heusler alloys is readily determined using x-rays diffraction techniques. The intensities of different lattice reflections are proportional to the square of the structure factor, F^2. For Heusler alloys, $F(111)$ and $F(200)$ correspond to the order-dependent superlattice reflections, while $F(220)$ is order-independent principal reflections.[3] Therefore, the different superlattices can be distinguished by comparing the intensity ratio of the different lattice reflection $I(111)/I(200)$. Here, two different structure models[30] as shown in Figs. 1(b) and 1(c) were considered. In an ordered $L2_1$ structure [Fig. 1(b)], Mn atoms occupy *A* and *C* sites. By exchanging the Mn at *C* sites and Ni at *B* sites, the $L2_1$ structure changes into another highly ordered structure with a different superlattice, shown in Fig. 1(c). In this paper, Mn_2NiGa denotes the stoichiometric compound. MnNiMnGa and MnMnNiGa, representing the basis along the diagonal direction in two unit cells, are used to distinguish the structures shown in Figs. 1(b) and 1(c), respectively. In other words, MnNiMnGa and MnMnNiGa have the same chemical composition and principal cubic structure, but are different superlattices, which can be detected by comparing the relative intensities of corresponding peaks in XRD spectrums.[3,31]

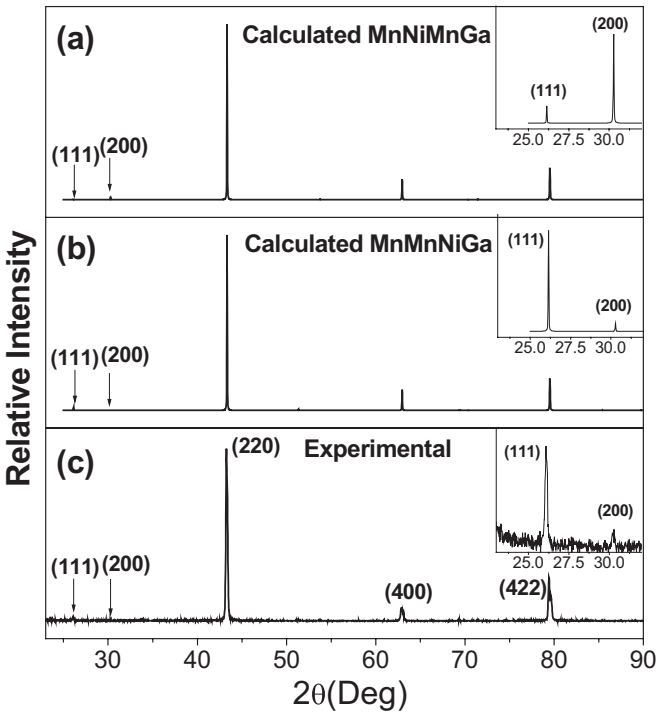

FIG. 2. Calculated x-ray powder diffraction patterns for cubic MnNiMnGa structure (a) and MnMnNiGa structure (b). The experimental pattern was shown in (c).

Figures 2(a) and 2(b) show the calculated XRD patterns for powder samples with the experimental lattice constant of $a=5.9072$ Å for MnNiMnGa and MnMnNiGa structures. As expected, they show quite different $I(111)/I(200)$ ratios, which is usually used to identify the structure in this intermetallic compound family.[31,32] The experimental XRD pattern for Mn_2NiGa powders is shown in Fig. 2(c), which clearly has the MnMnNiGa structure. This result is consistent with neutron diffraction for Mn_2NiSn.[30] The MnMnNiGa structure's prototype is Hg_2CuTi alloy and be-

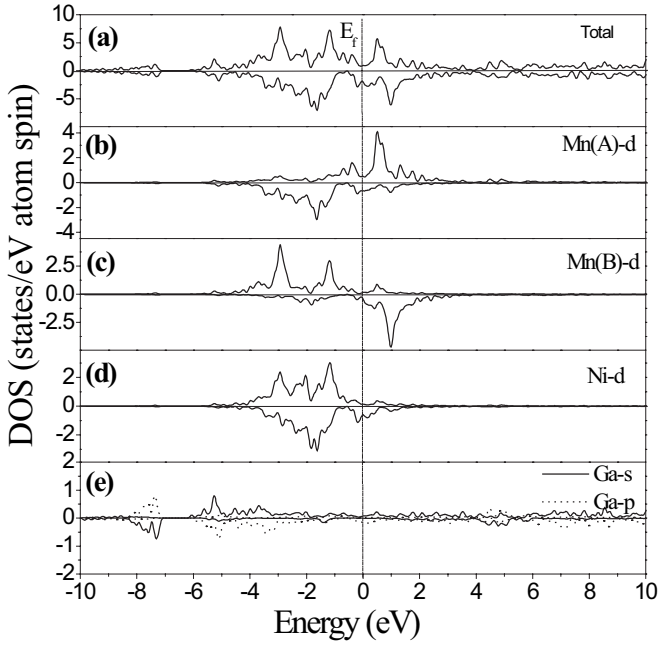

FIG. 3. Calculated spin-projected DOS plots for cubic MnMnNiGa structure. (a) The total DOS of Mn_2NiGa and the partial DOS of (b) d component of Mn(A) atoms, (c) d component of Mn(B) atoms, (d) d component of Ni atoms, (e) s and p component of Ga atoms. The upper halves of each panel display the spin-up states and the lower halves spin-down states.

longs to the $F\bar{4}3m$ space group, which is different from the $L2_1$ structure with $Fm\bar{3}m$ space group.[33,34]

Some Heusler alloys studied in the past have one Mn atom per formula unit cell and show an $L2_1$ structure. In contrast, the alloys with two Mn atoms per formula unit cell, and especially with MnMnNiGa structure, have rarely been studied. In this structure, these two Mn atoms sit in two different sublattices, which will show very different electronic and magnetic properties. With these in mind, we carried out the first-principles calculations to study the electronic structure and magnetism of MnMnNiGa.

B. Electronic structure and magnetism

1. MnMnNiGa and MnNiMnGa structures in austenite phase

In Heusler alloys, the magnetic properties can be altered by changing the degree or type of chemical order.[3] It is known that the Mn-Mn distance plays an important role here. The large Mn-Mn distances difference in MnNiMnGa (2.9536 Å) and MnMnNiGa (2.5579 Å) implies significantly different magnetic properties in these two types of structures. The total density of states (DOS) for MnMnNiGa using the experimental lattice constant of $a=5.9072$ Å is shown in Fig. 3(a). One strong peak for Ga atom at about −15.48 eV is not shown since it is symmetric between spin-up and -down states and therefore does not contribute to the total moment. For the majority-spin state, the DOS is very low near the Fermi level and only Mn at A sites [Mn(A)] have a slight contribution. For the minority-spin state, the DOS of Ni and Mn(A) dominate near the Fermi level. The 3d bands for Mn at B sites [Mn(B)] has a peak above the Fermi level in the spin-down states, and a double-peak structure in spin-up states below the Fermi level arising from the splitting of Mn e_g-t_{2g} levels in a cubic crystal field. The large splitting in DOS between spin-up and -down states suggests a strong exchange, which leads to large localized spin magnetic moments at the Mn(B) sites.[4] For Mn(A) atoms, the spin-down states are mostly situated below the Fermi level, while the spin-up bands shows a maxim above the Fermi level. It is also clear that the exchange splitting of Mn(A) d states is weaker than that of Mn(B) atoms in this alloy because of different local surrounding. The spin-up and -down d bands of Ni atoms are equally populated with negligible contributions to the total moment.

The Mn 3d bands are very different for the two spin directions and crucially depending on sites. The calculations clearly show the ferrimagnetism for MnMnNiGa with antiparallel magnetic moments between Mn(A) and Mn(B) atoms. The numbers for spin-up and spin-down 3d electrons on Mn(A) are 1.84 and 4.04, respectively, which leads to a magnetic moment of $-2.20\mu_B$. Considering the contribution from 4s and 4p electrons of $0.38\mu_B$, the total moment of Mn(A) is $-2.58\mu_B$ with an electronic configuration of $3d^{5.88}4s^{0.5}4p^{0.7}$. For Mn($B$) atoms, 4.40 and 1.25 electrons occupy the spin-up and spin-down states respectively, which lead to a magnetic moment of $+3.15\mu_B$ for 3d electrons. With additional moments from 4s and 4p electrons of $+0.19\mu_B$ and $+0.22\mu_B$, respectively, the total magnetic moment of Mn(B) is $+3.56\mu_B$ with an electronic configuration $3d^{5.65}4s^{0.64}4p^{0.78}$. The magnetic moments of Ni and Ga atoms are $+0.26\mu_B$ and $+0.04\mu_B$, respectively. The calculated total magnetic moment is $1.28\mu_B$ in Mn_2NiGa, which translates to 30.00 emu/g. The value is slight less than the experiment result of 31.43 emu/g to be presented later. All relative parameters of electronic structure calculated are summarized in Table I.

Mn(B) atoms in MnMnNiGa-type Mn_2NiGa occupy the same sites as Mn atoms in Ni_2MnGa. The magnetic moment of Mn(B) is 15% less than that of Mn atoms in Ni_2MnGa. This indicates that additional Mn atoms [Mn(A)] do affect the electronic structure of Mn(B) and reduces the magnetic moment of Mn(B) in Mn_2NiGa. It should also be noted that the Mn(A) atoms show much larger magnetic moments than Ni atoms at A site in Ni_2MnGa, and these moments are antiparallel to those of Mn(B), resulting in decreasing saturation magnetization in Mn_2NiGa compared with Ni_2MnGa. Similar phenomenon has also been observed in other Heusler alloys with high Mn content.[24,35]

Next, we discuss the total and d component of DOS (Fig. 4) for Mn_2NiGa with MnNiMnGa structure, where Mn atoms occupy A and C sites. The 3d bands are very similar for Mn(A) and Mn(C) and clearly show the ferromagnetic characteristics with parallel magnetic moments on these two sites. The similarity in DOS between Mn(A) and Mn(C) atoms is commonly observed in Heusler alloys due to their similar surroundings. The magnetic moment of Mn is $3.13\mu_B$ and the magnetic moments of Ni and Ga are 0.41 and $-0.26\mu_B$, respectively. The total magnetic moment is thus $6.41\mu_B$ in Mn_2NiGa, corresponding to 150.23 emu/g, which

TABLE I. The band calculation parameters, the charge distributions on the constituent atoms, the 3*d* magnetic moment on atoms μ_d, molecular magnetic moment M, exchange splitting ΔE_x, and ratio $I=\Delta E_x/\mu_d$ for Mn atoms in Mn_2NiGa intermetallic compound. The notations *s*, *p*, and *d* mean the components of the charges.

Structure	species	spin	*s*	*p*	*d*	μ_d (μ_B)	$M(\mu B)$	ΔE *x*	$I=\Delta E$ x/μ_d
MnGaNiMn	Mn(*A*)	↑	0.19	0.22	1.84	−2.20	1.28	2.1	0.95
		↓	0.31	0.48	4.04				
	Mn(*B*)	↑	0.42	0.50	4.40	+3.15		2.8	0.89
		↓	0.23	0.28	1.25				
	Ni	↑	0.29	0.52	4.52	+0.27			
		↓	0.30	0.52	4.25				
	Ga	↑	1.11	1.13	4.99	0.00			
		↓	0.10	1.12	4.99				
MnGaMnNi	Mn(*A*)	↑	0.26	0.41	4.39	+2.99	6.41	2.6	0.87
		↓	0.21	0.32	1.40				
	Mn(*B*)	↑	0.26	0.41	4.39	+2.99		2.6	0.87
		↓	0.21	0.32	1.40				
	Ni	↑	0.30	0.45	4.70	+0.68			
		↓	0.42	0.60	4.02				
	Ga	↑	0.12	1.02	5.00	0.00			
		↓	0.13	1.27	5.00				
MnGaNiMn	Mn(*A*)	↑	0.30	0.37	3.63	+1.38	1.41	1.3	0.94
Martensite		↓	0.23	0.30	2.25				
	Mn(*B*)	↑	0.32	0.35	2.91	−0.01			
		↓	0.32	0.36	2.92				
	Ni	↑	0.30	0.49	4.36	−0.04			
		↓	0.33	0.51	4.39				
	Ga	↑	0.08	1.11	4.99	0.00			
		↓	0.08	1.12	4.99				

is inconsistent with our experimental results to be presented later. This result confirms that Mn_2NiGa alloy favors the MnMnNiGa structure instead of the MnNiMnGa structure. The fact that the calculated total magnetic moment is slightly less than the experimental value can be reasonably attributed to the small amount of Mn atoms antisitting between *A* and *B* sublattices. In addition, the total energy calculated with experimental lattice constants for MnNiMnGa type is 0.44 eV/cell higher than that of MnMnNiGa-type structure and the structure is therefore less favorable.

It was believed that the magnetism, especially in 3*d* alloys, is predominantly determined by the immediate environment around potentially magnetic atoms. One has to consider four aspects of short-range order to understand the magnetism: the number, type, distance, and symmetry of the nearest neighbors about a given site.[36] Comparing Fig. 1(b) with Fig. 1(c), in MnMnNiGa structure, a Mn(*A*) atom is surrounded by four Ga and four Mn(*B*) atoms, and a Mn(*B*) atom is surrounded by four Ni and four Mn(*A*) atoms. In contrast, all Mn atoms in a MnNiMnGa structure have a similar environment, and each is surrounded by four Ga and four Ni atoms. Due to the difference in local environment, it is expected that Mn(*A*) and Mn(*B*) in MnMnNiGa have very different moments, whereas all Mn atoms in MnNiMnGa structures carry the same moments (Table I).

To describe the magnetic ordering of Heusler alloys, three types of interactions are usually considered: (1) superexchange via the *sp* electrons of Ga atoms; (2) s-d_{Mn} interaction between the *s* conduction electrons and the localized d_{Mn} electrons via a Ruderman-Kittel-Kasuya-Yosida (RKKY) type exchange; and (3) *d*-*d* interaction which leads to a common *d* band with rather delocalized *d* electrons.[37] Although these interactions intermingle and complicate the interpretation, the final ordering seems to be only a function of the nearest Mn-Mn distance. The smaller separation among Mn(*A*) and Mn(*B*) in MnMnNiGa gives rise to antiferromagnetic coupling between Mn(*A*) and Mn(*B*) sublattices, and large separation among Mn atoms, which is the case in MnNiMnGa structure and within each sublattice of Mn(*A*) and Mn(*B*), lead to ferromagnetic coupling. Therefore, for the same composition ofMn_2YZ (where *Y* and *Z* are other transition metal elements and *s*-*p* elements, respectively), the magnetic properties will sensitively depend on the Mn loca-

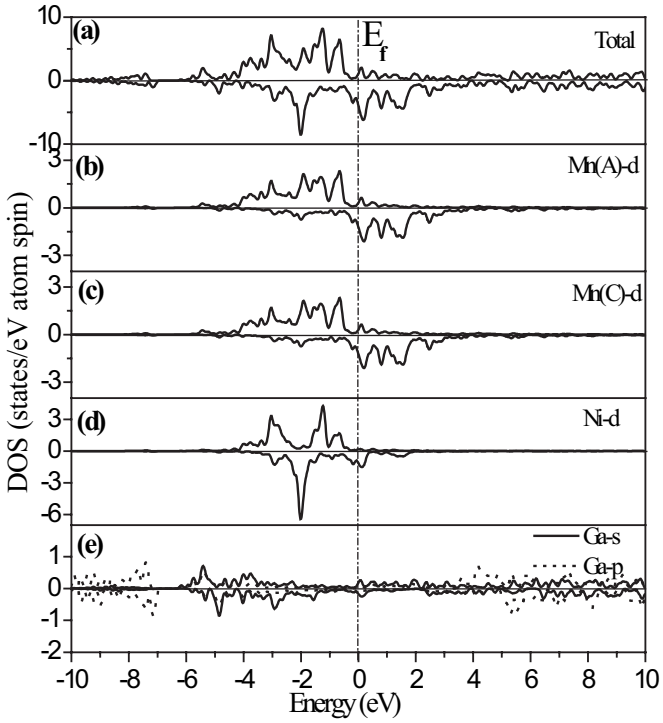

FIG. 4. Calculated spin-projected DOS plots for cubic MnNiMnGa. (a) The total DOS of Mn_2NiGa and the partial DOS of (b) d component of Mn(A) atoms, (c) d component of Mn(C) atoms, (d) d component of Ni atoms, (e) s and p component of Ga atoms. The upper halves of each panel display the spin-up states and the lower halves spin-down states.

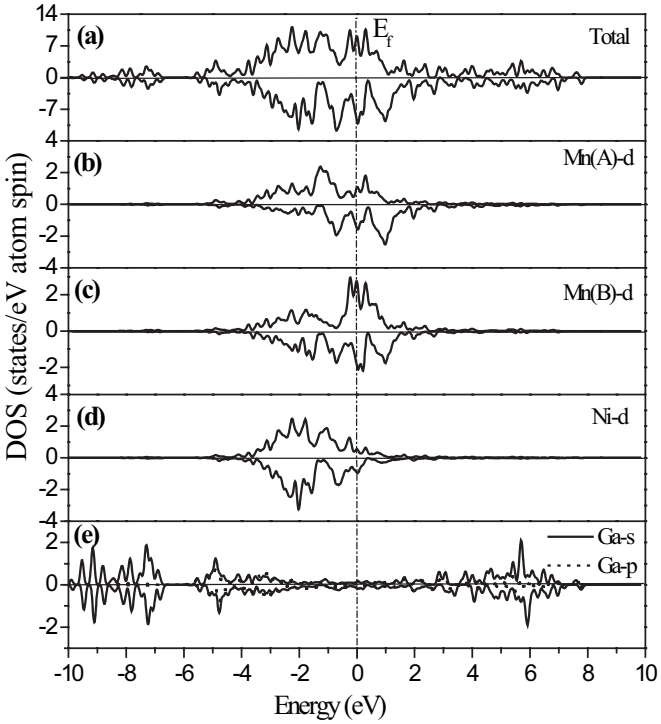

FIG. 5. Calculated spin-projected DOS plots for tetragonal MnMnNiGa. (a) The total DOS of Mn_2NiGa and the partial DOS of (b) d component of Mn(A) atoms, (c) d component of Mn(B) atoms, (d) d component of Ni atoms, (e) s and p component of Ga atoms. The upper halves of each panel display the spin-up states and the lower halves spin-down states.

tions. Based on this knowledge, one may manufacture similar materials with rich physical properties.

2. MnMnNiGa structures in martensite phase

In our previous report,[26] Mn_2NiGa undergoes a martensitic transformation from a cubic to a tetragonal structure. We thus calculated the electronic structure and magnetic moment of Mn_2NiGa alloys in a tetragonally distorted MnMnNiGa lattice. The experimental lattice constants determined by XRD are $a=b=5.5472$ Å and $c=6.7144$ Å and are used in this calculation. Figure 5 shows the calculated DOS. Similar to previous discussions, we omit the major DOS for Ga atom at about −15.48 eV. The electron states from Mn and Ni are found to have the largest contributions to the total DOS. The distinct feature in this structure is that most states for Mn(A) and Mn(B) are near the Fermi level and have a large overlap. The strong hybridization between Mn(A) and Mn(B) weakens the intra-atomic exchange interaction. Correspondingly, the polarization of 3d electrons is also weakened and the magnetic moment of the Mn atom decreases. The total number of the 3d spin-up and spin-down electrons does not change for Mn atoms. As shown in Table I, the numbers of spin-up and spin-down 3d electrons on Mn(A) are 3.63 and 2.25, respectively, leading to a magnetic moment of $1.38\mu_B$. For Mn(B) atoms, the numbers are 2.91 and 2.92 for spin-up and spin-down electrons, respectively, giving rise to a magnetic moment of $-0.01\mu_B$. Taking into account the contributions of other electrons and atoms, the total calculated magnetic moment is $1.41\mu_B$ per formula unit of Mn_2NiGa, corresponding to 33.28 emu/g. It is only slightly less than our experiment result of 33.49 emu/g.

The symmetry plays an important role on magnetism and broken symmetry will reduce the band degeneracies.[36] The intra-atomic exchange interaction between Mn 3d electrons can be expressed in terms of the semi-empirical relation $J=0.59+0.075(Z-21)$, which gives Mn atoms ($Z=25$) a value of $J=0.89$ eV. If intra-atomic exchange interactions are the origin of the exchange splitting between spin-up and spin-down bands, one expects $I=\Delta E_x/\mu_d$ to be equal to J.[38,39] The exchange splitting ΔE_x has been listed in Table I. The fact that the values of I obtained from band-structure calculations are very close to the atomic parameter J proves that the exchange splitting between Mn 3d bands is mainly an intra-atomic effect. Comparing Figs. 3 and 5, the DOS indicates that the Mn 3d bands are much more localized in energy for austenite than martensite, which indicates the important influence of the crystal symmetry.[40] Therefore, the intra-atomic exchange interaction of Mn atoms was seriously tampered, especially for Mn(B) atoms whose moments are suppressed to zero. For the Mn(A) atoms, ferromagnetic alignment was induced by the indirect exchange interaction.

3. General discussion

By comparing their band structures, one can see there are very different hybridizations in cubic MnMnNiGa and

MnNiMnGa austenite and tetragonal MnMnNiGa martensitic structure, which are important to explain the interatomic exchange interactions.[37] In cubic MnMnNiGa structure, the moments on Mn(A) and Mn(B) are antiparallel and the hybridization between Mn(A) and Mn(B) $3d$ electrons are weak because of small overlap of states at similar energy level. Therefore, the antiparallel alignment between Mn(A) and Mn(B) sublattices was maintained by a weak direct $d_{\mathrm{Mn}(A)}$-$d_{\mathrm{Mn}(B)}$ exchange interaction. The ferromagnetic coupling within each sublattice is stabilized by the s-d_{Mn} interaction via s electrons in Mn or Ga atoms. In cubic MnNiMnGa structure, the Mn(A) and Mn(C) are not the nearest-neighboring atoms and the indirect exchange should be considered as the main exchange mechanism. In the martensite case, the hybridization between different Mn sublattices is much stronger, leading to the formation of a broader d band in the martensite. The interatomic interaction is so strong that the intra-atomic interaction is almost completely suppressed. Only Mn(A) atoms have a remaining moment of $1.44\mu_B$, which are aligned in parallel by the indirect exchange.

Comparing the above-calculated results for Ni_2MnGa, it becomes clear that the Mn atoms that substituted Ni have much larger magnetic moments than those of the original Ni atoms, but are antiparallel to those of the original Mn atoms. Upon the martensitic transformation, the Ni_2MnGa shows a small increase in magnetization due to the small increase of moments of Ni atoms and Mn atoms which are largely intact during the transformation. The reason can be attributed to the large Mn-Mn distance in both martensite and austenite. However, for Mn_2NiGa, although the magnetization also show a small increase, the magnetic moments of Mn(A) and Mn(B) atoms changes dramatically. In Mn_2NiGa, the Mn(A) and Mn(B) are nearest neighbors and much closer than that in Ni_2MnGa. Therefore, after the structural transition, the hybridization between Mn(A) and Mn(B) atoms can be strongly influenced with much reduced moments. The small increase in magnetization is attributed to the counteractive changes in moments of Mn(A) and Mn(B) atoms.

C. Experimental results

In this section, we present our experimental results to reveal how the magnetism changes when Ni_2MnGa is gradually transferred into Mn_2NiGa with a substituting process. The original sample has a composition of Ni_2MnGa was chemically changed by increasing Mn and decreasing Ni content simultaneously to achieve a series of samples denoted as $Ni_{2-x}Mn_{1+x}Ga$ (x=0.2, 0.4, 0.5, 0.6, and 0.8). The magnetizations for the various compositions were measured at 5 K and are shown in Fig. 6(a). As reported previously, all the samples have a cubic structure at high temperature and undergo a martensitic transformation to a tetragonal structure at low temperatures.[26]

Figure 6(b) shows the composition dependence of the magnetic moment per formula unit. The moments decrease linearly with increasing Mn content, and follow the expression $M_x = M_0 - \Delta M \times x$ where M_x is the magnetic moment of $Ni_{2-x}Mn_{1+x}Ga$, ΔM is the moment change when one Ni atom

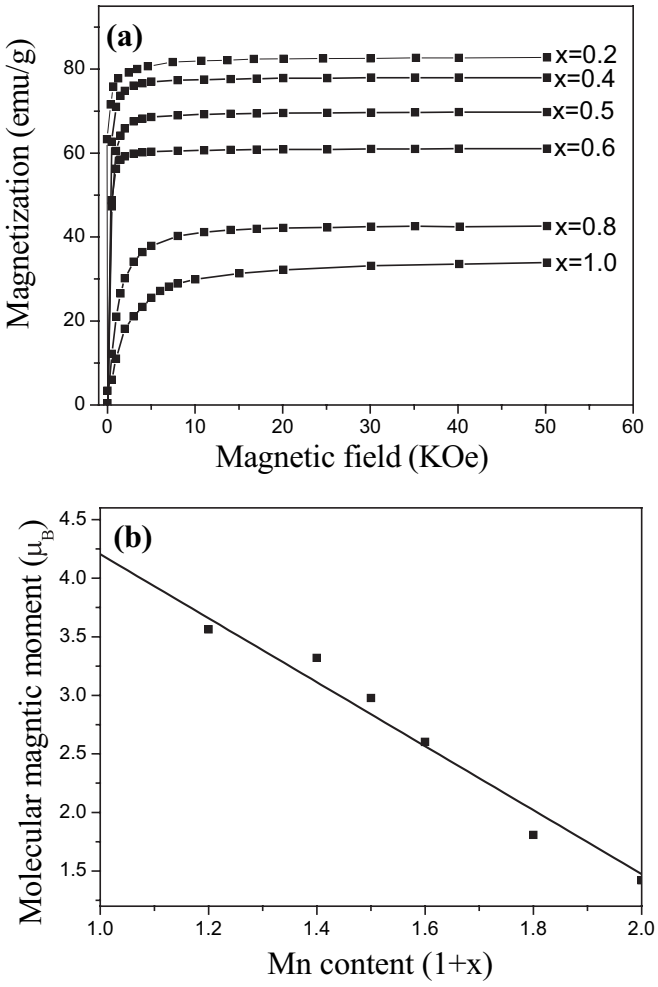

FIG. 6. (a) The magnetic field dependence of magnetization for $Ni_{2-x}Mn_{1+x}Ga$ at 5 K. (b) Magnetic moment as a function of Mn content (1+x) in $Ni_{2-x}Mn_{1+x}Ga$ system measured at 5 K in a field of 5 T.

was substituted by one Mn atom and x is the composition variable. The best fitting yields $M_0 = 4.20\mu_B$ and $\Delta M = 2.72\mu_B$. This extrapolates to $4.20\mu_B$ for Ni_2MnGa, which is quite consistent to the reported experimental value of $4.17 \pm 0.20\mu_B$.[3] The ΔM value of $2.72\mu_B$ is also in agreement with the experimental value of $2.73\mu_B$. This means that, going from Ni_2MnGa to Mn_2NiGa by substituting Ni atoms at the A site with Mn atoms, the additional Mn atoms take the same magnetic structure as in Mn_2NiGa martensite. This observation can be extended to the austenite phase. Unlike in martensite phase above, Mn(B) atoms in austenite carry sizable moment which are antiparallel to that of Mn(A). The number of Mn(A) atoms is gradually increasing during the substituting process and is finally equal to the number of Mn(B) atoms in Mn_2NiGa. Consequently, all off-stoichiometric samples $Ni_{2-x}Mn_{1+x}Ga$ show a coexistence of ferromagnetic order due to uncompensated Mn(B) atoms and ferrimagnetic order between Mn(A) and Mn(B) sublattice, which is consistent with results reported by J. Enkovaara.[24]

The temperature dependence of magnetization from 5 K to 600 K in a 5 T magnetic field is shown in Fig. 7 for Mn_2NiGa. One can see that the Curie temperature is 588 K,

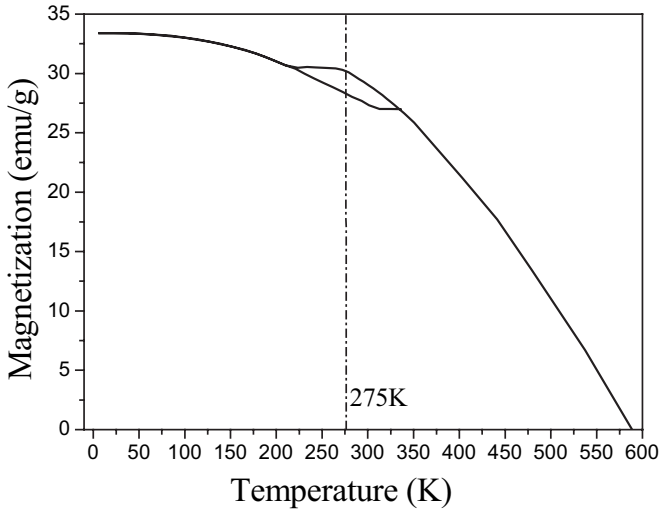

FIG. 7. Temperature dependence of the saturation magnetization M_S for 5 K $< T <$ 600 K.

which is consistent with our previous report where the Curie temperature was determined by measuring ac susceptibility.[26] In single-phase martensite or austenite, magnetization decreases smoothly and monotonically with increasing temperature. The magnetization decreases upon martensitic transformation. Comparing the magnetization of austenite with that of martensite at 275 K (at this temperature, the material is austenite upon cooling but it is martensite upon heating), the material has nearly a 10% reduction in magnetization from austenite to martensite. This behavior is quite similar to that in a Ni-Mn-Sn system, but differs from that in Ni_2MnGa where the magnetization of martensite is higher than that of the parent phase. We should note that, in our calculated results (at 0 K), the magnetic moment in martensite is larger than that in austenite, which is in contrast to the experimental results observed at 275 K. As discussed in previous sections, the material has different magnetic ordering in martensite and austenite. Especially, the austenite show ferrimagnetism due to antiparallel but unbalanced magnetic moments of Mn atoms at *A* and *B*sublattices. Usually, the ferrimagnetic materials show complex temperature dependence in magnetization due to the competition between two different sublattices, each with different magnetic moment. Therefore, this problem may be attributed to the different temperature dependence due to the different magnetic ordering for martensite and austenite. We are currently investigating this mechanism.

IV. CONCLUSION

The Mn_2NiGa alloy favors MnMnNiGa structure with *A* and *C* sublattices occupied by Mn and Ni atoms, respectively, instead of MnNiMnGa structure with both *A* and *C* sublattices being occupied by Mn atoms. The Mn_2NiGa alloy exhibits a complex magnetic behavior due to the high content of Mn and their atomic order. Although, experimentally, there are no significant changes in magnetization between martensite and austenite phase, the calculated electronic structure reveals very different magnetic properties. The material is ferrimagnetic in austenite due to the antiparallel but unbalanced moments for Mn atoms at different sublattice. The magnetic moment of Mn atom decrease greatly upon martensitic transformation to a tetragonal structure with a 50% reduction in Mn(*A*) moments to about $1.44\mu_B$ and almost completely suppressed Mn(*B*) moments. The material shows a ferromagnetic characteristic in martensite phase. This might imply an applied magnetic field could have a strong influence on martensitic transformation, which deserves further investigation. At low temperatures, the spontaneous magnetization of Mn_2NiGa at martensite is larger than that at austenite because of antiferromagnetic coupling in austenite. Different magnetic orderings in martensite and austenite also lead to very different temperature dependence, with which the abnormal behavior of magnetization upon martensitic transformation can be understood. For the samples with composition $Ni_{2-x}Mn_{1+x}Ga$, the process of magnetic change with increasing Mn content has been presented experimentally. It is believed that in the off-stoichiometric samples, the additional Mn atoms play the same role as that in the Mn_2NiGa.

ACKNOWLEDGMENT

This work is supported by the Key Project of the National Natural Science Foundation of China Grant No. 50571113.

[1] F. Heusler, W. Starck, and E. Haupt, Verh. Dtsch. Phys. Ges. **5**, 220 (1903).
[2] P. J. Webster and R. S. Tebble, J. Appl. Phys. **39**, 471 (1968).
[3] P. J. Webster, Contemp. Phys. **10**, 559 (1969).
[4] J. Kübler, A. R. Williams, and C. B. Sommers, Phys. Rev. B **28**, 1745 (1983).
[5] K. Ullakko, J. K. Huang, C. Kantner, R. C. O'Handley, and V. V. Kokorin, Appl. Phys. Lett. **69**, 1966 (1996).
[6] A. Fujita, K. Fukamichi, F. Gejima, R. Kainuma, and K. Isshida, Appl. Phys. Lett. **77**, 3054 (2001).
[7] M. Wuttig, J. Li, and C. Craciunescu, Scr. Mater. **44**, 2393 (2001).
[8] K. Oikawa, L. Wulff, T. Iijima, F. Gejima, T. Ohmori, A. Fujita, K. Fukamichi, R. Kainuma, and K. Ishida, Appl. Phys. Lett. **79**, 3290 (2001).
[9] O. Heczko, N. Glavatska, V. Gavriljuk, and K. Ullako, Mater. Sci. Forum **373**, 341 (2001).
[10] M. Matsumoto, T. Takagi, J. Tani, T. Kanomata, N. Muramatsu, and A. N. Vasil'ev, Mater. Sci. Eng., A **273**, 326 (1999).
[11] A. Vasil'ev, A. Bozhko, V. Khovailo, I. Dikshtein, V. Shavrov, S. Seletskii, and V. Buchelnikov, J. Magn. Magn. Mater. **196&197**, 837 (1999).
[12] C. H. Yu, W. H. Wang, J. L. Chen, G. H. Wu, F. M. Yang, N. Tang, S. R. Qi, W. S. Zhan, Z. Wang, Y. F. Zheng, and L. C.

Zhao, J. Appl. Phys. **87**, 6292 (2000).
[13] S. J. Murray, M. Marioni, S. M. Allen, and R. C. O'Handley, Appl. Phys. Lett. **77**, 886 (2000).
[14] R. W. Overholser and M. Wuttig, Scr. Mater. **40**, 1095 (1999).
[15] A. A. Likhachev and K. Ullakko, Phys. Lett. A **275**, 142 (2000).
[16] Aparna Chakrabarti, C. Biswas, S. Banik, R. S. Dhaka, A. K. Shukla, and S. R. Barman, Phys. Rev. B **72**, 073103 (2005).
[17] N. Lanska, O. Söderberg, A. Sozinov, K. Ullakko, and V. K. Lindroos, J. Appl. Phys. **95**, 8074 (2004).
[18] V. A. Chernenko, E. Cesari, V. V. Kokorin, and I. N. Vitenko, Scr. Metall. Mater. **33**, 1239 (1995).
[19] A. N. Vasil'ev, A. D. Bozhko, V. V. Khovailo, I. E. Dikshtein, S. G. Shavrov, V. D. Buchelnikov, M. Matsumoto, S. Suzuki, T. Takagi, and J. Tani, Phys. Rev. B **59**, 1113 (1999).
[20] V. A. Chernenko, Scr. Mater. **40**, 523 (1999).
[21] I. Dikshtein, V. Koledov, V. Shavrov, A. Tulaikova, A. Cherechuking, V. Buchelnikov, V. Khovailo, M. Matsumoto, T. Takagi, and J. Tani, IEEE Trans. Magn. **35**, 3811 (1999).
[22] L. Mañosa and A. Planes, Adv. Solid State Phys. **40**, 36 (2000).
[23] X. Jin, M. Marioni, D. Bono, S. M. Allen, R. C. O'Handley, and T. Y. Hsu, J. Appl. Phys. **91**, 8222 (2002).
[24] J. Enkovaara, O. Heczko, A. Ayuela, and R. M. Nieminen, Phys. Rev. B **67**, 212405 (2003).
[25] F. Zuo, X. Su, P. Zhang, G. C. Alexandrakis, F. Yang, and K. H. Wu, J. Phys.: Condens. Matter **11**, 2821 (1999).
[26] G. D. Liu, J. L. Chen, Z. H. Liu, X. F. Dai, G. H. Wu, B. Zhang, and X. X. Zhang, Appl. Phys. Lett. **87**, 262504 (2005).
[27] E. Wimmer, H. Krakauer, M. Weinert, and A. J. Freeman, Phys. Rev. B **24**, 864 (1981).
[28] M. Weinert, E. Wimmer, and A. J. Freeman, Phys. Rev. B **26**, 4571 (1982).
[29] J. Rath and A. J. Freeman, Phys. Rev. B **11**, 2109 (1975).
[30] R. B. Helmholdt and K. H. J. Buschow, J. Less-Common Met. **128**, 167 (1987).
[31] Y. Feng, J. Y. Rhee, T. A. Wiener, D. W. Lynch, B. E. Hubbard, A. J. Sievers, D. L. Schlagel, T. A. Lograsso, and L. L. Miller, Phys. Rev. B **63**, 165109 (2001).
[32] Mehmet Acet, Eyup Duman, Eberhard F. Wassermann, Lluis Mańosa, and Antoni Planes, J. Appl. Phys. **92**, 3867 (2002).
[33] M. Puselj and Z. Ban, Croat. Chem. Acta **41**, 79 (1969).
[34] P. Villars and L. D. Calvert, *Pearson's Handbook of Crystallographic Data for Intermetallic Phases*, 2nd ed. (ASM International, Materials Park, Ohio, 1991), p. 2868.
[35] T. Krenke, E. Duman, M. Acet, E. F. Wassermann, X. Moya, L. Manosa, and A. Planes, Nat. Mater. **4**, 450 (2005).
[36] R. C. O'Handley, *Modern Magnetic Materials: Principles and Applications* (Wiley, New York, 1999), p. 165.
[37] S. Picozzi, A. Continenza, and A. J. Freeman, Phys. Rev. B **66**, 094421 (2001).
[38] D. van der Marel and G. A. Sawatzky, Phys. Rev. B **37**, 10674 (1988).
[39] J. H. Wijngaard, C. Haas, and R. A. de Groot, Phys. Rev. B **45**, 5395 (1992).
[40] Y. J. Zhao, W. T. Geng, A. J. Freeman, and B. Delley, Phys. Rev. B **65**, 113202 (2002).